PROCEEDINGS, 47th Workshop on Geothermal Reservoir Engineering
Stanford University, Stanford, California, February 7-9, 2022
SGP-TR-223

Examination of the Enhanced Thermal Conductivity Effect by the Induced Convective Heat Flux in a Fractured Thermal Reservoir on Closed-loop Geothermal Energy Production Technology

Gang Zhao[1], Wanju Yuan[2], Zhuoheng Chen[2], Chang Su[3]

[1]University of Regina, 3737 Wascana Parkway, Regina, SK S4S 0A2

gang.zhao@uregina.ca

[2]Geological Survey of Canada, Natural Resources Canada, 3303 33rd street NW, Calgary, Alberta, T2L 2A7

wanju.yuan@NRCan-RNCan.gc.ca

zhuoheng.chen@NRCan-RNCan.gc.ca

[3]China National Offshore Ocean Corporation Limited-Shanghai, 200000 Shanghai, China

suchang4@cnooc.com.cn

Keywords: Closed-Loop geothermal technology, induced convective flow, reservoir modeling, enhanced thermal conductivity, fractured thermal reservoir

ABSTRACT

Closed-loop geothermal energy recovery technology is one of the promising methods to produce the heat energy from thermal reservoirs. This technology is independent of geothermal reservoir permeability, greatly reducing the exploration risk, and there exist no associated environmental and scaling issues that are usually accompanying the production of geothermal fluids to surface. A key limitation in this technology though is that the heat in a closed-loop system can only be produced from reservoir by heat conduction across the wellbore. The overall thermal conductivity is normally considered constant as the fluids in the reservoir are assumed static during the temperature change. However, there will happen some locally induced convective flow in the near wellbore region due to fluids density change caused by surrounding temperature reduction. This kind of induced heat convection will enhance the heat transfer process in the near wellbore region and eventually improve the heat production performance of a closed-loop system. This study builds two dimensional and three dimensional models to demonstrate that the induced convective flow will enhance the overall thermal conductivity in fractured or highly permeable thermal reservoirs. The results show that a significant convective flow induced velocity improvement can be observed in the region near the horizontal wellbore, with the spherically shaped convective flow likely spreading outskirts, mainly in the vertical downward lower region, for the cases with higher permeability. The naturally induced convective flow velocity has a significant increase for the permeability range of 1.0 D ~ 10.0 D. Note that this result also suggests that only heavily fractured thermal reservoir becomes sufficiently supportive to take the advantage of density-driven convective flow.

1. INTRODUCTION AND RELATED LITERATURE REVIEW

Geothermal resource is proved to be a clean, renewable and reliable energy deriving from the heat dynamically stored in Earth's subsurface. While geothermal hot springs and associated by-products such as mineral have been used since antiquity, only in the early 20th century did people start to consider the natural heat from inside the Earth as a particular source of energy where electricity was first generated at Larderello, Italy (World Energy Council, 2013). Geothermal energy has now been utilized to produce electric power, building heat, and other commercial purposes such as grain drying, paper processing, greenhouse and soil warming (International Geothermal Association, 2021). Canada has numerous potential geothermal resources, it is estimated that Canada's in-place geothermal power exceeds one million times Canada's current electrical consumption (Grasby et al., 2011), however, no geothermal electrical production has been successfully implemented in Canada so far.

A practical technology called closed-loop system or geothermal heat exchanger is widely applied in heat extraction for building heating and some projects aims at power generation (**Fig. 1**) (Eavor, 2022). It circulates water or supercritical CO_2 (GreenFire, 2022) in a closed system to extract heat out of the ground. Because there is no fluid communication hydraulically, it has less footprint on environment and less operational cost. However, the heat extraction efficiency by this technology is frequently questioned because heat could only be transferred to pipes by heat conduction mechanism. The formation thermal diffusivity, associated with thermal conductivity, plays a crucial role for the successful application of this technology.

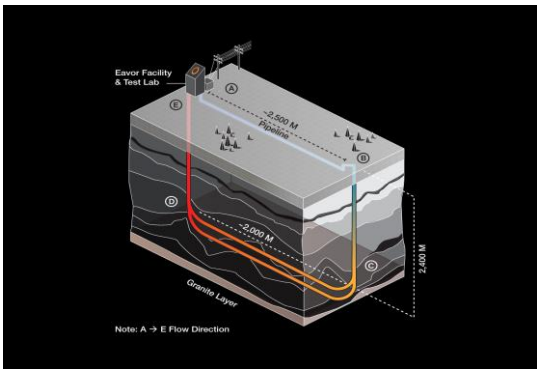

Figure 1: Eavor-Loop demonstration project illustration (Eavor, 2022).

The evaluation of formation thermal conductivity is one of the most important works in the feasibility study of closed-loop geothermal energy production project (Dalla Santa et al., 2020). If the mean thermal conductivity cannot be accurately predicted, even the most sophisticated and appropriate modeling techniques for analyzing thermal histories and organic maturation levels may fail when applied to real basins (Blackwell and Steele, 1989). Currently, the techniques of thermal conductivity measurement are mainly based on two categories, Laboratory Techniques and In Situ Techniques.

Laboratory Techniques. Most values of thermal conductivity for rocks come from measurements made on samples in the laboratory. Typical measurement techniques include the needle-probe transient measurement suitable for use on very soft materials and cuttings (**Fig. 2**a), and the divided-bar steady-state measurements suitable for use on consolidated core and some cuttings samples (Fig. 2b). The needle-probe technique generally is to insert a long needle into the rock or soil installed with a heater wire and a thermal sensor. When the heater is turned on, a temperature history is recorded from which the thermal conductivity can be captured. For divided-bar methods, an axial heat flux is applied to a saturated sample and the associated temperature drop is imposed across the thickness of the sample. The temperature drop is then further compared to standard materials, such as quartz and silica glass, so a relative thermal conductivity can be obtained.

In Situ Techniques. There are direct measurements and indirect measurements to obtain *In Situ* thermal conductivity values. The main philosophy is to insert a tool into a hole and measure the transient heat transfer performance based on the dynamic temperature change. A number of different types of indirect methods have been proposed. These include correlation of various well-log parameters with thermal conductivity, correlation of reflection two-way travel times with thermal resistance, and calculation of thermal conductivity from temperature-gradient logs. These indirect methods are largely applied in geothermal exploration phase.

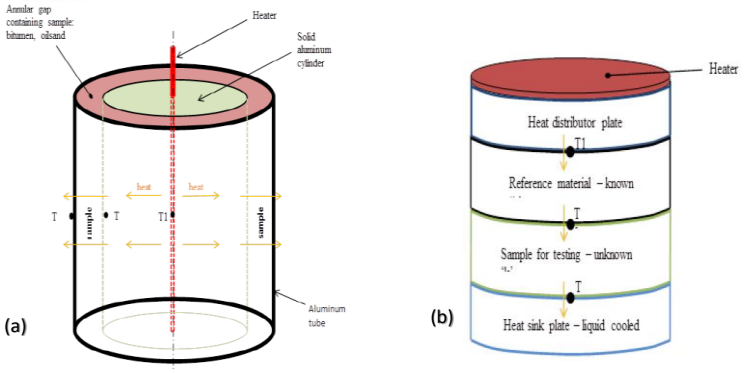

Figure 2: Illustration of a) needle-probe transient measurement; b) divided-bar steady-state measurement (PERM Inc., 2021).

During the practical heat production process, the density of reservoir fluids near wellbore will be changed due to the local temperature decreasing. The induced density-driven natural convectional flow process will occur, and this regional heat convection near wellbore can increase the overall heat transfer efficiency. As a result, an effective thermal conductivity, or pseudo-thermal conductivity, could be higher than the value estimated from labs or correlations. Over the years, density-driven free convection phenomena have been analyzed by numerical, laboratory, and field experiments on groundwater studies including seawater intrusion in coastal aquifers, leachate infiltration from waste disposal, salt lakes and saline disposal basins, with interaction between groundwater and surface water (Frind, 1982; Huyakom et al., 1987; Kooi et al., 2000; Micheael et al., 2016; Schincariol and Schwartz, 1990; Shincariol et al., 1994; Simmons and Narayan, 1997; Stevens et al., 2009; Van Dam et al., 2009). Reservoir heterogeneity with different permeability inclusion was proved to have an impact on free convection in porous medium (Yan et al., 2019). Taking heat transfer into consideration, salinization in a stratified aquifer induced by heat transfer from well casings has been evaluated for gas, oil and geothermal energy production activities (van Lopik et al., 2015). In geothermal energy production process of closed-loop system, better heat production performance is possible where thermal and

hydraulic conductivities are higher (Rees et al., 2004; Oldenburg et al., 2016). Permeability larger than 1 mD or even reaching to 100 D will significantly improve the heat recovery efficiency by the closed-loop system (Oldenburg et al., 2016; Beckers et al., 2022).

The Geological Survey of Canada (GSC) is conducting multiple research projects aiming at comprehensive geothermal resources assessment, advanced geothermal energy production technologies, and geothermal energy co-production with the Carbon Capture, Utilization and Storage (CCUS) activities. The closed-loop geothermal energy production technology has been demonstrated in Alberta, Canada and has good potential to be applied in western Canada. This study focuses on analytical and numerical studies of the impact of induced convective flow on overall reservoir thermal conductivity when water flow through a sealed horizontal production tube in a fractured igneous basement reservoir. This work firstly discussed the theoretical study and physics consideration on this problem. A simplified analytical model has been proposed to preliminarily evaluate the impact of steady convective heat transfer on pseudo-thermal conductivity estimation. Two different numerical methods, finite difference method (FDM) and finite element method (FEM), have been applied to study the same process. All simulation studies show a significant enhancement on pseudo-thermal conductivity by induced convective heat transfer in a highly permeable porous media setting.

2. THEORETICAL STUDY AND CONSIDERATIONS

The induced density-driven heat convection contains multiple physical processes. The cold working fluid flows within a sealed horizontal pipe completed in a high temperature formation with good thermal conductivity. The heat is transferred through the wellbore wall to the working fluid flowing inside wellbore, and then the heated fluid is produced out through vertical wellbore. Due to the large fluid velocity inside the pipe, heat convection process dominates the heat transfer performance along the fluid flow direction. Previous researches usually assume pure heat conduction mechanism outside the pipe, where the heat is transferred from higher temperature reservoir bulk body to lower ones, with no fluid flow inside the formation considered, thus leading to a pure conductive heat process without any convective flow involved. However, in reality the fluid in the reservoir nearby wellbore will actually experience heat loss to the pipe, causing its density to increase and certain degree of thermal phase shrinking will happen too. **Fig. 3** illustrates that a fluid element nearby the pipe is losing its heat, and then its temperature decreases with an associated density increase and volume shrinkage. Therefore, a corresponding fluid flow will happen based on these mechanisms.

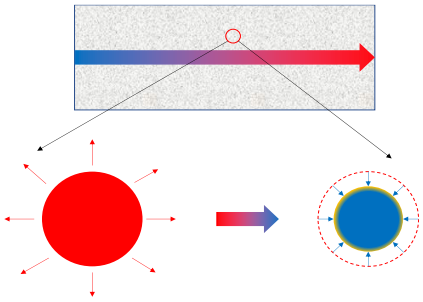

Figure 3: Illustration of a fluid element losing the heat and having a volume shrink.

Due to the physics of heat transfer diffusivity, this kind of induced density-driven convection flow will only occur in the near-wellbore region. The fluid near the pipe will firstly lose its heat to wellbore and gain certain amount of density increase and volume shrinkage. Higher fluid density will result in its own downward flow. The left volume and shrined volume will be occupied by higher temperature fluids coming mainly from upward fluid. The fluid with slightly light density in the lower position will then moving upward from sideways. The total process will form a natural density-driven convection flow region near the heat production pipe, which will enhance the efficiency of heat transfer to closed-loop system (**Fig. 4**). Except applicable to hot dry rock, sedimentary basins usually have good permeability and porosity, as well as natural fractures or induced fractures near the wellbore. All these features will enhance the induced density-driven flow near a closed-loop system within the reservoir. It is conceivable that this kind of induced density-driven convection flow will be more important for a long term geothermal well production practice, especially for geothermal reservoirs with larger thickness, higher permeability and increasing temperature difference to encourage convective fluid flow vertically.

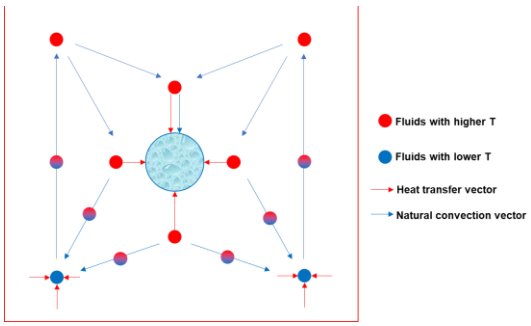

Figure 4: Illustration of the induced density-driven natural convection near the sealed pipe.

3. ANALYTICAL SOLUTIONS ON THEORETICALLY SIMPLIFIED CASE

In order to support the understanding and evaluation of the contribution of the induced convective flow in geothermal production process, this study built a simplified physical model with a novel mathematical model and applied analytical method to investigate this process. A typical near pipe region has been chosen to study the heat transfer process (**Fig. 5**). The heat is transferred to pipe by conduction at and through the wall of the pipe. There assumes a continuous fluid flow from upward region to downward region. Heat conduction and convection both affect the overall heat transfer performance simultaneously. This theoretical model can be regarded as a combined model that integrates one dimensional heat conduction and convection processes systematically.

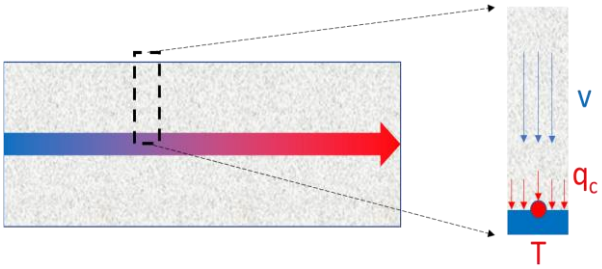

Figure 5: Illustration of the simplified model using in analytical modeling method.

3.1 Assumptions

Several reasonable assumptions have been made for this simplified theoretical model.

1. The induced density-driven fluid convection has a steady velocity flowing from outside reservoir towards the wall of pipe.

2. The heat extraction rate, or the heat out flow, at the wall of pipe is assumed to be a constant rate, considering the total heat extraction duty will be stable during the operation years by working fluid flow control.

3. The fluid and rock matrix are in temperature equilibrium for any instantaneous heat source/sink change.

4. Thermal properties and hydraulic properties remain constant during the temperature change.

3.2 Methodology

This study applied a patent-pending technology (Zhao et al., 2021) to treat heat convection process as a contribution of an additional source through conduction, with its strength dynamically and integratively specified in modeling process. The point function of instantaneous heat source or sink can be mathematically described as Eq. 1 and Eq. 2 (Carslaw and Jaeger, 1959; Newman, 1936).

$$\Delta T(x,x',t,\tau) = \frac{1}{A\rho c}\int_0^t \frac{q(\tau)}{2\sqrt{\pi\alpha\,(t-\tau)}}\, exp\left(-\frac{(x-x\prime)^2}{4\alpha\,(t-\tau)}\right) d\tau \tag{1}$$

$$\alpha = \frac{\lambda}{\rho c} \tag{2}$$

where, ΔT is the temperature change,℃; q is the continuous heat rate injected or produced from a 2D infinite heat domain, J/s; α is the heat diffusivity, m^2/s; x and x' are the corresponding locations of the evaluation point and the source/sink point, m; A is the source area, m^2; t is the time and τ represents the moment in time when a source occurs, so $(t\text{-}\tau)$ stands for the elapsed time since a source occurs. With Laplace transformation, and Stehfest inverse method (Stehfest, 1970), the temperature change for the thermal domain at certain time point can be obtained.

Based on the physics of heat convection, heat convection is idealized as a special case of conduction process, with its source strength specified by the bulk movement of fluids. This kind of source function, therefore, can be described using Eq. 3.

$$\Delta T_v(x,x',t,\tau) = \frac{\rho_f c_f}{\rho c}\int_0^t v_{x\prime}(\tau)\frac{\partial T}{\partial x\prime}(\tau)\cdot\frac{dx\prime}{2\sqrt{\pi\alpha\,(t-\tau)}}\, exp\left[-\frac{(x-x\prime)^2}{4\alpha\,(t-\tau)}\right] d\tau \tag{3}$$

Where, ΔT_v is the temperature difference made by convective heat flux, ℃; the upper quotation mark indicates the parameter for source; x is the evaluation point location.

With the approximation of uniform strength for heat convective source within each sub-segment, the convective heat source could be written as Eq. 4.

$$\Delta T_v(x,y,t) = \frac{\rho_f c_f}{\rho c}\int_0^t v_x(\tau)\frac{\partial T}{\partial x}(\tau)\cdot\left\{\frac{1}{2}erf\left[\frac{x_2-x}{2\sqrt{\alpha(t-\tau)}}\right]-\frac{1}{2}erf\left[\frac{x_1-x}{2\sqrt{\alpha(t-\tau)}}\right]\right\}d\tau \quad (4)$$

Where, x_1 and x_2 denote the starting and ending points of the sub-segment region, respectively.

3.3 Validation

This proposed model for convection heat transfer is validated by two commercial numerical simulation packages. The first validation work is conducted by a fine gridded numerical simulation by COMSOL simulator on a standard 1D heat convection case. The basic parameters used in validation case are listed in Table 1.

Table 1: Parameters used in validation case.

Parameter	Symbol	Value	Unit
System length	L	50	m
Segment size	L_s	1	m
Density-driven flow velocity	v	0.005	m/day
Heat outflow flux rate	q_o	5	W/m^2
Thermal conductivity of rock	λ_r	3.5	W/m/K
Thermal conductivity of fluid	λ_f	0.6	W/m/K
Rock density	ρ_r	2500	kg/m^3
Fluid density	ρ_f	1000	kg/m^3
Heat capacity of rock	c_{pr}	1100	J/kg/K
Heat capacity of fluid	c_{pf}	4180	J/kg/K
Porosity	φ	0.3	1
Initial reservoir temperature	T_i	120	˚C

Fig. 6 shows the results of temperature at different distance to the pipe after 1 year heat production. It is observable that a good match with the result calculated by COMSOL heat transfer in porous media module. Actually, this method has been also validated under different boundary and initial conditions by numerical simulations and other analytical solutions (Yuan, 2020).

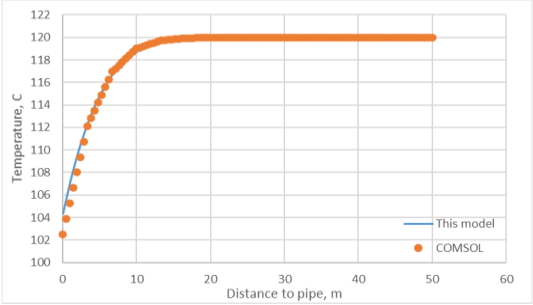

Figure 6: Temperature profile at different distance to the pipe after 1 year heat production.

The second validation case is a thermodynamic modeling of a typical conventional geothermal energy production case by a doublet-well system, shown in **Fig. 7.** A cold water injection well and a hot water production well were set to have the same flow rate. The initial reservoir temperature is 200 ^{o}C, and the cold injected water temperature is maintained at 35 ^{o}C. The temperature distributions are calculated by the method proposed in section 3.2 and the commercial numerical software CMG STARS module. The results at 30 days were plotted in **Fig. 8**. The outcomes of the temperature distributions are very close to each other. Two temperature profiles along the red dashed straight lines shown were presented in **Fig. 9** (left figure, the red dashed vertical line) and **Fig. 10** (left figure, the red dashed horizontal line), where the figures on the right hand side show the results generated by these two methods are consistent with each other. However the numerical model requires a much fine-meshed scheme.

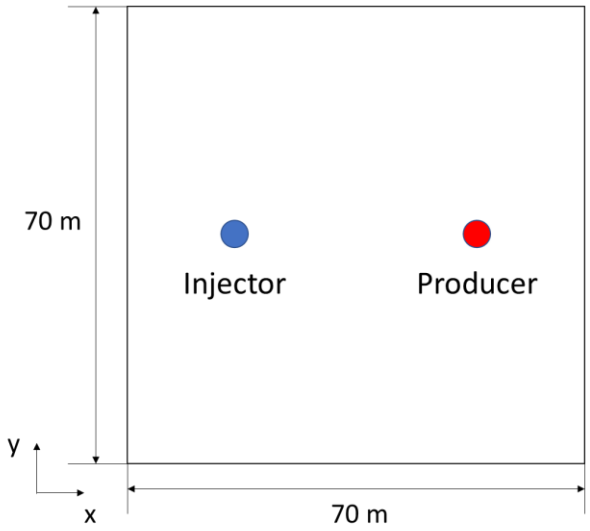

Figure 7: Diagram for the model setting of the second validation case.

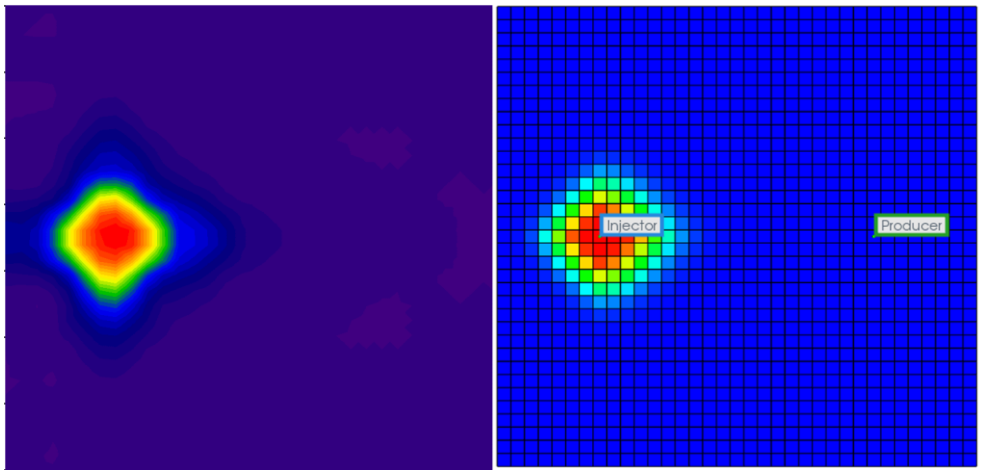

Figure 8: Temperature change distributions at 30 days for the two methods (left: this method; right: CMG STARS).

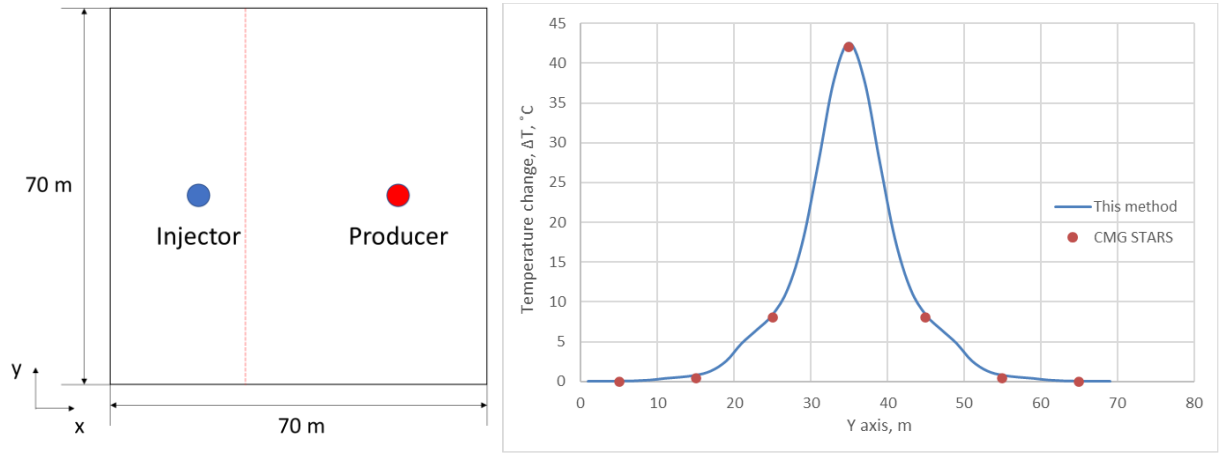

Figure 9: Temperature change profile along a straight line (the red dashed vertical line).

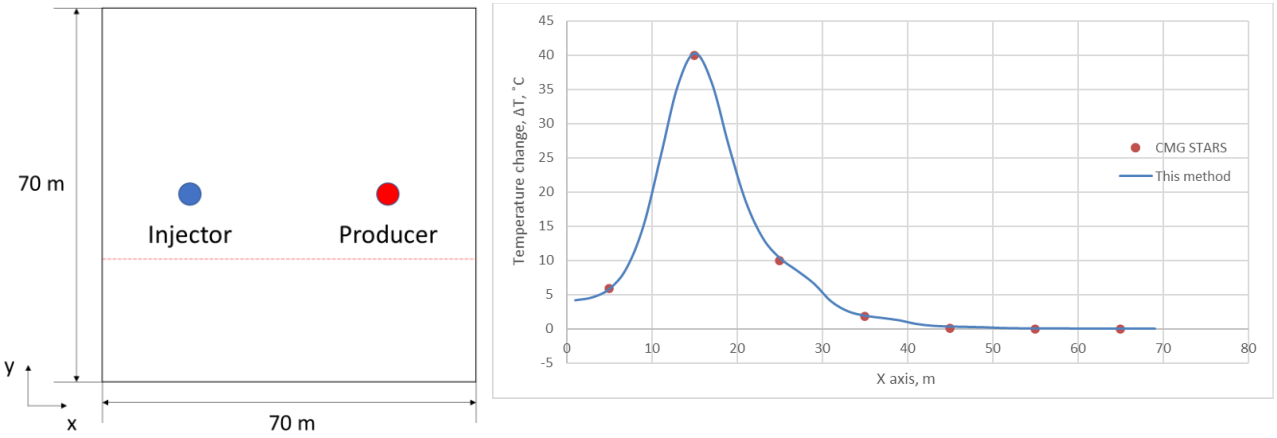

Figure 10: Temperature change profile along a straight line (the red dashed horizontal line).

3.4 Discussion

The induced density-driven convection accelerates the heat transfer performance within the region near the heat production pipe. This kind of enhancement could be evaluated through defining an equivalent pseudo-thermal conductivity term, λ_{pseudo}, for having the same temperature change response. For pseudo-thermal conductivity calculation, only pure thermal conduction is considered in the heat transfer process. Then, the ratio of the pseudo-thermal conductivity to the actual thermal conductivity (λ) of the original system is defined as λ_E to indicate the degree of pseudo-thermal conductivity enhancement at different production time.

$$\lambda_E = \frac{\lambda_{pseudo}}{\lambda} \tag{5}$$

Five different density-driven velocity values have been studied to calculate the pseudo-thermal conductivity and their corresponding enhancement. These velocity values are mainly determined by fluid-reservoir system diffusivity, pressure change, and existing natural fracture structure.

The results of thermal conductivity enhancement by density-driven convection velocity are shown in **Fig. 11.** The thermal conductivity enhancement is not constant throughout the energy production process. It keeps increasing and showing significant heat transfer enhancement in later energy production phase. Higher density-driven convection velocity will result in more significant enhancement at later production phase. This result indicates that the consideration of convective flow is important, especially under the condition of higher conductive flow velocity. The empirical functions of the enhancement under different convective flow velocity could be generated by the following polynomial equations:

$$\lambda_E = 1\text{E-}07t^5 - 9\text{E-}06t^4 + 0.0003t^3 - 0.005t^2 + 0.0668t + 1.2494, \text{ v=0.001 m/day} \tag{6}$$

$$\lambda_E = 2\text{E-}07t^5 - 1\text{E-}05t^4 + 0.0005t^3 - 0.0085t^2 + 0.1367t + 1.3147, \text{ v=0.002 m/day} \tag{7}$$

$$\lambda_E = 2E\text{-}07t^5 - 2E\text{-}05t^4 + 0.0007t^3 - 0.0114t^2 + 0.2202t + 1.3789,\ v=0.003\ m/day \quad (8)$$

$$\lambda_E = 3E\text{-}07t^5 - 3E\text{-}05t^4 + 0.0009t^3 - 0.013t^2 + 0.3186t + 1.4416,\ v=0.004\ m/day \quad (9)$$

$$\lambda_E = 3E\text{-}07t^5 - 3E\text{-}05t^4 + 0.0009t^3 - 0.0128t^2 + 0.4325t + 1.5027,\ v=0.005\ m/day \quad (10)$$

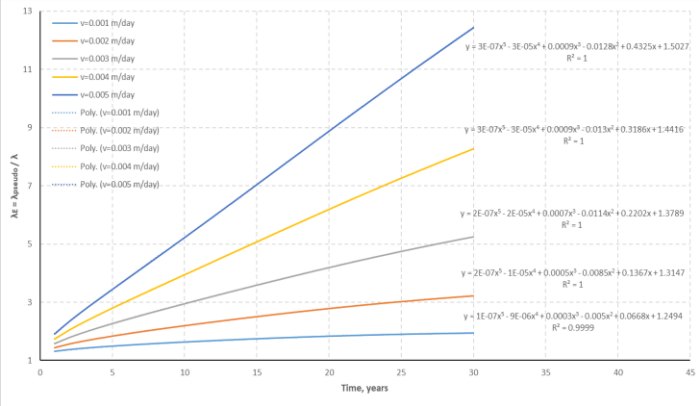

Figure 11: Results of pseudo-thermal conductivity enhancement under different density-driven convective velocity.

3.4 Consideration of fractured thermal reservoir modeling

The modeling technology for complicated fractured thermal reservoir is still a very challenging task presently, especially when a fracture network near wellbore is considered, thus further efforts dedicating to this target will be conducted based on the general framework and theoretical understanding of Zhao et al (2021). For this work, in order to address the main concern of the density-driven convective flow process and generate a fundamental understanding of the overall effect of fracture rock mass on the common thermal fluid flow process, a large-scale reservoir permeability variation over a range of 0.001mD ~ 10D is studied. This large change enables a clear view of the enhanced density-driven convective flow due to the supporting effect of higher equivalent permeability enhanced by natural fracture network for fluid flow. This is especially true for heavily fractured rocks. Future work will be implementing advanced fracture simulation strategy to deal with natural fracture networks and stimulated reservoir volume (SRV) concept of the enhanced geothermal system (EGS) for geothermal reservoir development.

4. NUMERICAL MODELING USING FINITE DIFFERENCE METHOD

4.1 CMG Model setup

CMG STARS module was used to analyze the density-driven convection effect on closed-loop geothermal energy production system. The reservoir depth is around 2400 m. The geothermal gradient and gravity effect are considered in this model. The well configuration and reservoir view are shown in **Fig. 12.** The reservoir blocks near the horizontal wellbore have an initial uniform temperature of 200 ˚C. The initial reservoir temperature and pressure can be seen as **Fig. 13.** Other parameters are listed in **Table 2.**

Table 2: Parameters used in finite difference method simulator.

Parameters	Symbol	Value	Unit
Length of the lateral pipe	L	550	m
Circulating rate	q	50	m^3/day
Porosity	φ	1	%
Thermal conductivity of rock	λ_r	3	W/m/K

Thermal conductivity of water	λ_f	0.65	W/m/K
Rock volumetric heat capacity	$\rho_r c_{pr}$	2.35e6	J/(m^3*K)
Water 1st thermal expansion coefficient	CT1	0.000417911	1/°C
Initial temperature at production layer	T_i	200	°C

There are some CMG specifics for the modeling of U-shape closed-loop geothermal energy production, attached here for reference:

1. Two FlexWells: one injector and one producer (both with an L shape).

2. Straight line relative permeability curves are used at the grid block where both wells have a perforation open.

3. There exists a 2nd thermal rock type for the block where the injector and producer FlexWells are connected. Rock heat capacity in this block remains the same and thermal conductivity changes to a smaller value to represent wellbore cement environment, following the requirement of FlexWells. Since this block is supposed to mimic a portion of a real wellbore, the thermal properties need to be adjusted here to reflect the wellbore reality.

4. In order to retain energy gained by the working fluid all the way up to surface, insulation needs to be applied to the producer well. If this is not done, most of the energy gained by the working fluid during the first vertical and the horizontal section will be transferred to the surrounding formations on the way to the surface. This applies to both simulation work and real operational scenarios.

5. In his model, working fluid injection and heat production were occurring from the same grid block (so there is no direct "connecting" block between them) but it is still required to model both wells. If modelling the "connecting" block is actually conducted, it still needs to have a straight-line relative permeability curve and very high permeability to mimic the wellbore fluid dynamics. The formation transmissibility factors will also have to be adjusted to a much higher value so as to effectively eliminate the communication of these blocks/cells with the rest of the reservoir, to build a wellbore closed to reality. Also, thermal properties of these blocks have to be adjusted to account for the heat loss from this "wellbore'' to the surrounding formation. Local grid refinement (LGR) needs to be done on the horizontal wellbore section in order to reduce the size of the local grid segments that contain the wellbore, which is basically represented by a "connecting" block/cell.

6. Finally, two water components (one initially inside the reservoir as the reservoir water and another one as the injected working fluid inside the wellbore) to make sure the correct components and phase initialization.

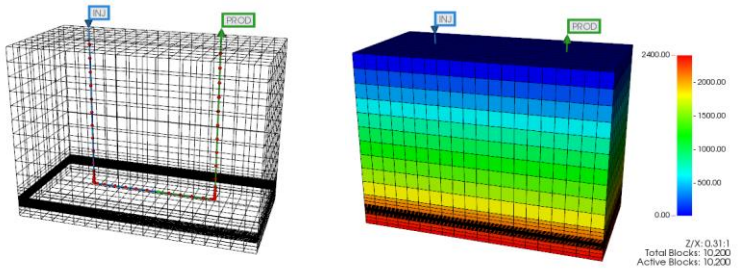

Figure 12: Well configuration (left) and reservoir setup (right) in numerical model.

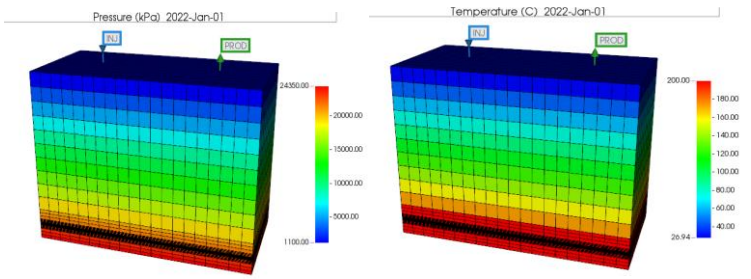

Figure 13: Initial reservoir pressure (left) and temperature (right).

4.2 Results

Three different permeability values near the horizontal wellbore region have been investigated in this study. The near wellbore region is defined as shown in **Fig. 14.** The results of outlet temperature over operation years are plotted in **Fig. 15.** The outlet temperature in the case with 100 Darcy permeability is the highest, whereas the outlet temperature in the case with lowest 0.001mD permeability have the lowest temperature value, especially in the late production phase the outlet temperature difference is more significant. However, the temperature increases from the case with 0.001 mD to the case with 1 D is not obvious. The reason may be that the corresponding induced density-driven velocity is not significant enough to induced effective temperature change as the permeability is not adequate. Because CMG cannot output the effective velocity value of the induced convective flow, likely due the fact that the velocity is very small. More details about this velocity will be shown in the next section when COMSOL software is applied. As the porosity increases from 1% to 30%, the overall outlet temperature decreases slightly (**Fig. 16**) because the overall thermal diffusivity decreases due to the existence of more pore volume, allowing fluid to hold up the heat contained.

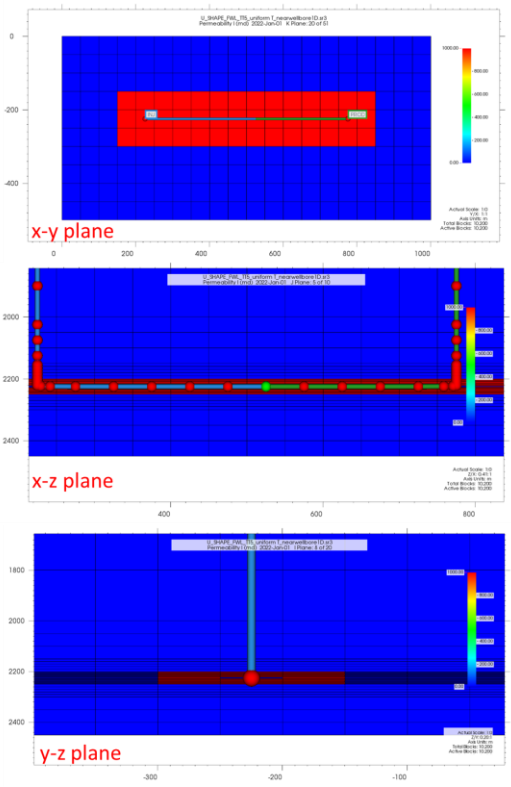

Figure 14: Permeability distribution in the region near horizontal wellbore.

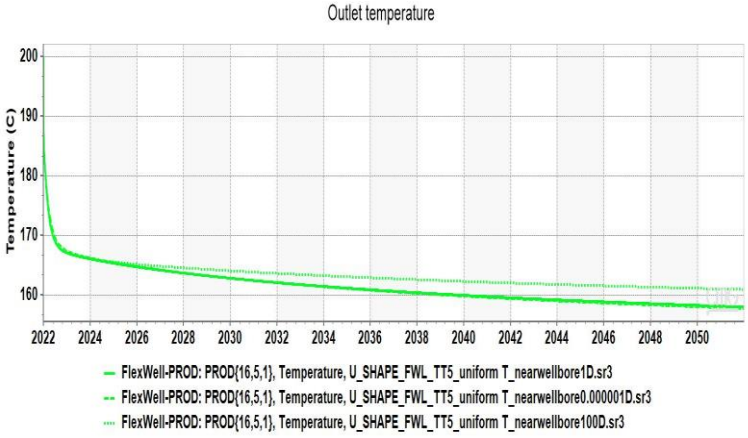

Figure 15: Outlet temperature for cases with 1% porosity and different permeability values in the near wellbore region.

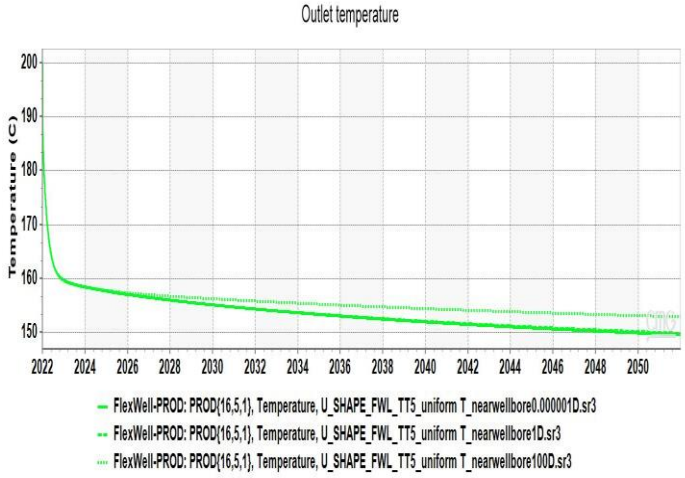

Figure 16: Outlet temperature for cases with 30% porosity and different permeability values in the near wellbore region.

5. NUMERICAL MODELING USING FINITE ELEMENT METHOD

Because the CMG STARS module cannot show the velocity profile in the modeling process, another fully coupled Thermal-Hydraulic-Mechanical-Chemical simulator, COMSOL, applying finite element method, is used to investigate the problem.

5.1 2D COMSOL model setup

A 2D model has been built to study the density-driven heat convection process during a constant heat production process at the center of the system (**Fig. 17**a). This is a cross-section view of the closed-loop lateral wellbore. The mesh graphic is shown in Fig. 17b. The model is a square shape system with a size of 100 m by 100 m, which denotes a near wellbore region. The other parameters use the same value listed in Table 1. The temperature values calculated for the thermal domain is used in pressure domain to calculate the density-driven Darcy's flow velocity, and the velocity is then applied into the thermal domain for heat convection calculation.

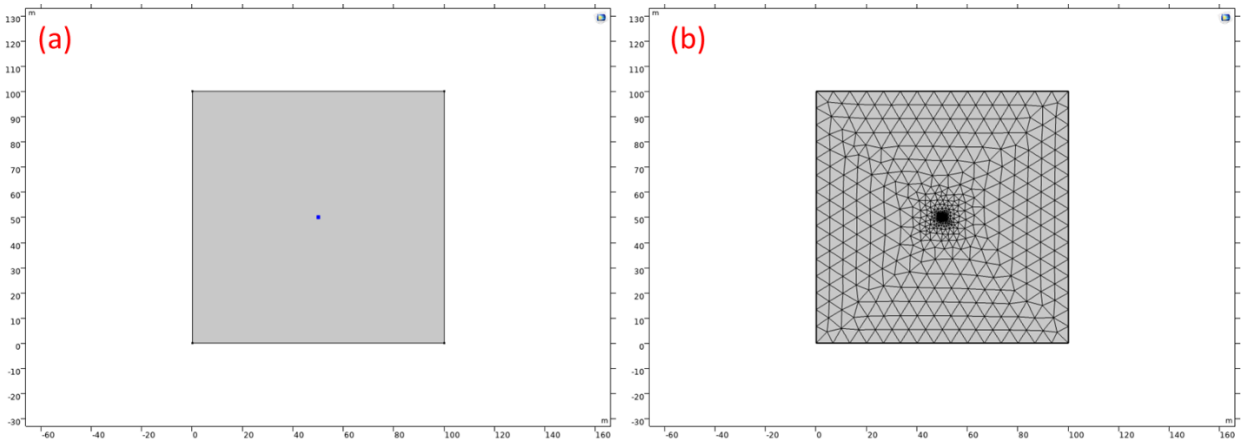

Figure 17: A 2D model of the closed-loop geothermal energy production system, a) the cross-section view; b) the mesh graphic.

5.2 2D Model results

Three different permeability values (10 mD, 1 D, 10 D) have been investigated in this 2D model. **Fig. 18** shows the temperature distributions of the cases at 24 years under different permeability values. The temperature distribution in the case with 10 mD is more symmetric in each direction, showing the dominant conductive flow scenario with the highest temperature values in the three cases. When the permeability increases, the overall reservoir temperature decreases. And the region below the wellbore have more temperature decrease, showing the contribution of the induced convective flow. **Fig. 19** shows the pressure distribution and convection flow velocity streamline of the cases with the three different permeability values at a 30-year time point. Because there are no conventional hydraulic source/sink in the system, the pressure level remains stable throughout the heat production process. Due to density change and fluid volume shrink, the induced density-driven convective flow occurs naturally and the velocity streamlines can be seen clearly to reflect the direction of the flow. The convective flow starts from the horizontal wellbore and moves toward down below, and then it will flow upward to form a circle loop due to the gradual phase warming up as it moves downward. When the permeability increases, the velocity of streamline shows more intensely below the horizontal wellbore, representing significant induced natural convective flow.

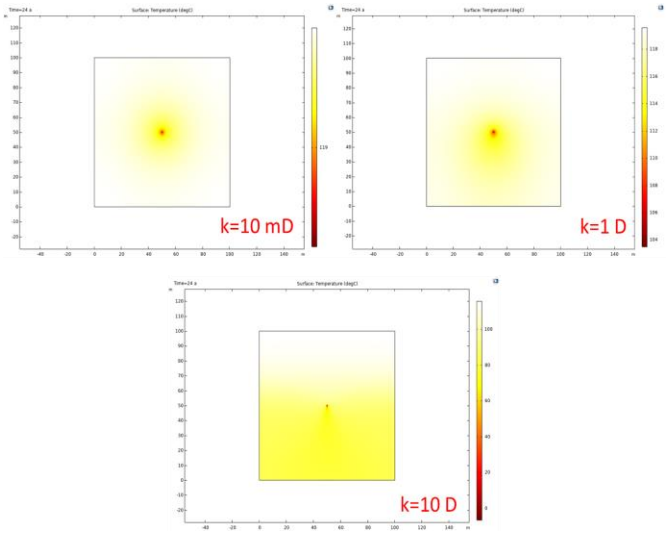

Figure 18: Temperature distributions of the cases with three different permeability values at 24 years.

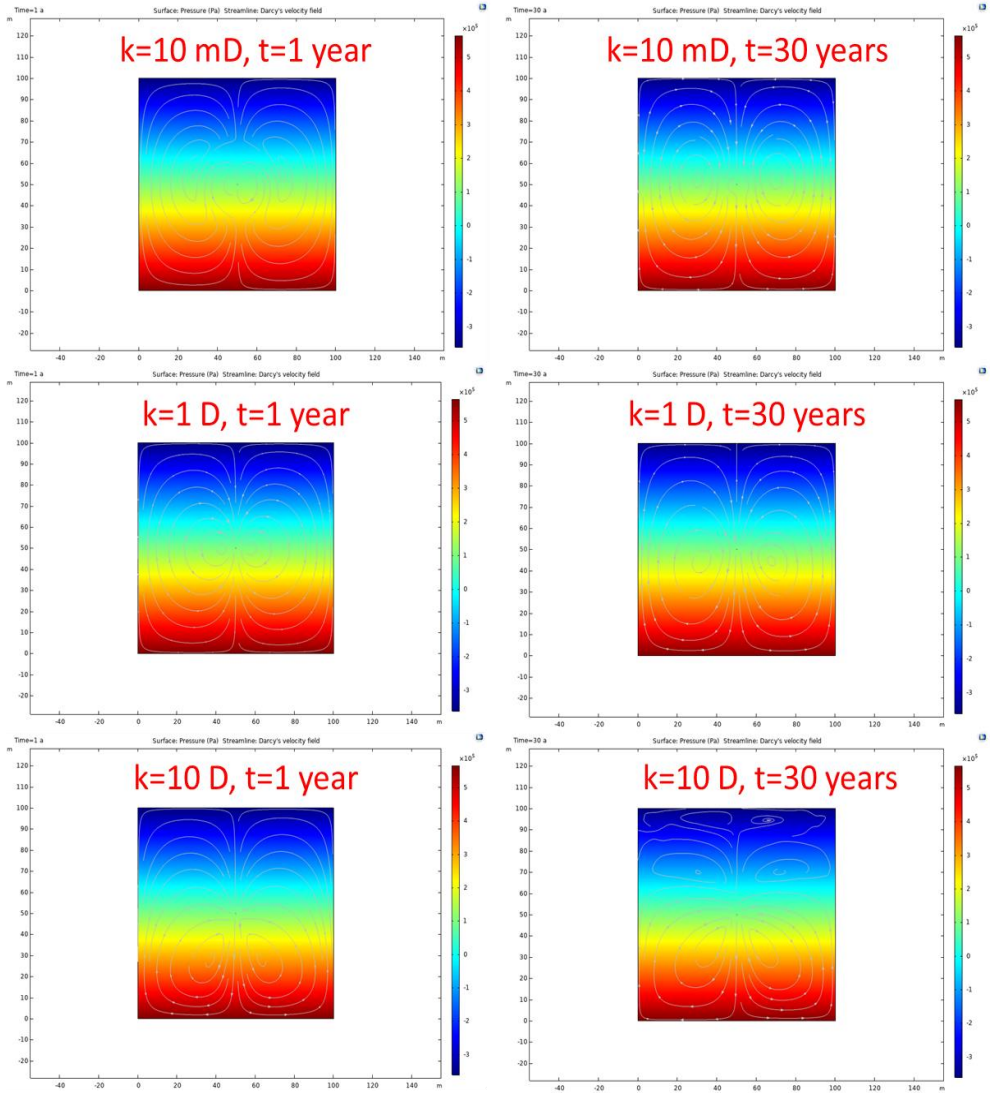

Figure 19: Pressure distribution and velocity streamlines of the cases with three different permeability values.

5.3 3D COMSOL model setup

A 3D model has been built to study the density-driven heat convection process during a closed-loop geothermal energy production system (**Fig. 20**b). The meshed graphic is shown in Fig. 20a. The model has a 500 m long horizontal pipe as the heat sink in the system. The other parameters use the same value in Table 1. These physics are studied in the model including heat transfer in porous media, Darcy's flow in porous media, and heat transfer in pipes. These three physics are fully coupled using COMSOL finite element method. The temperature distribution calculated for thermal domain is used in pressure domain to calculate the density-driven Darcy's flow velocity, and the velocity is then applied into the thermal domain for heat convection calculation. The heat transferred from reservoir to the wall of pipe will be the source for the heat transfer in the pipe.

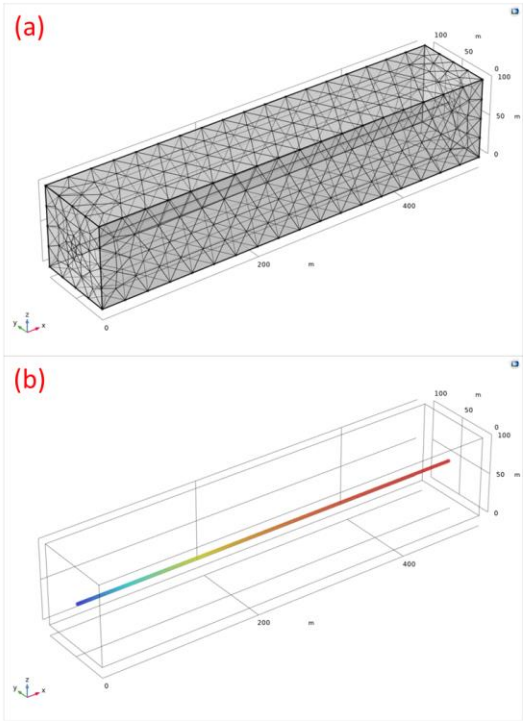

Figure 20: A 3D COMSOL model, a) the mesh graphic of the model; b) the closed-loop geothermal energy production system.

5.4 3D Model results

Three different permeability values (10 mD, 1 D, 10 D) have been investigated in this 3D model. **Fig. 21** shows the temperature distributions from cross-section view and 3D view of the case with 10 mD permeability. Because of the nature of the finite element numerical method, the temperature profiles are not smooth but still can show the temperature distribution features. The temperature change is symmetric in each direction. **Fig. 22** shows the velocity distributions and the convective flow direction. The velocity with 10 mD permeability is small and in the range of $1.0x10^{-10}$ to $1.0x10^{-9}$ m/s. The region near the wellbore has the most significant density-driven velocity, which denotes the significant temperature change in that area. As the permeability increases to 1 D. More temperature reduction shows in the region below the horizontal wellbore, shown in **Fig. 23**. And more velocity streamlines show in the lower region of the system (**Fig. 24**). It proves that higher permeability results in server density-drive convective flow and more amount of fluid is likely lose its heat and flows downward. The velocity increase is not that much compared with the case with 10 mD permeability. This may explain why outlet temperature does not increase much from 0.001 mD to 1 D in CMG numerical simulation results. When it comes to 10 D permeability case, most significant temperature drop can be observed in 2D and 3D distribution figures (**Fig. 25**). And the velocity also increases largely to the range of $1.0x10^{-7}$ to $1.0x10^{-6}$ m/s (**Fig. 26**).

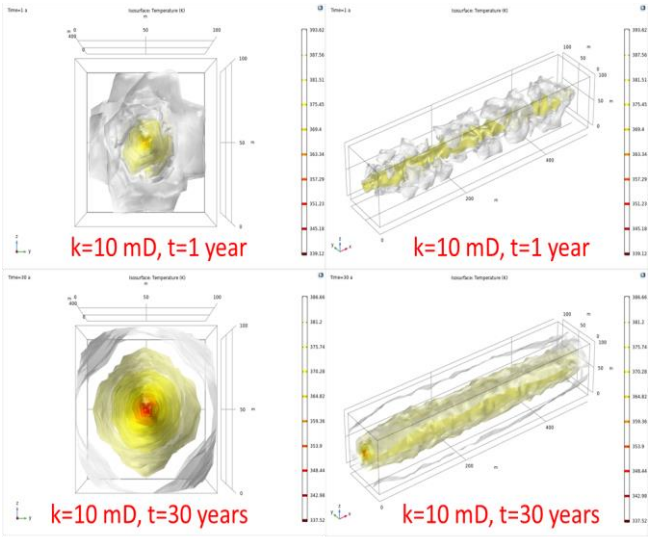

Figure 21: Temperature distribution at 1 year and 30 years of the case with 10 mD permeability.

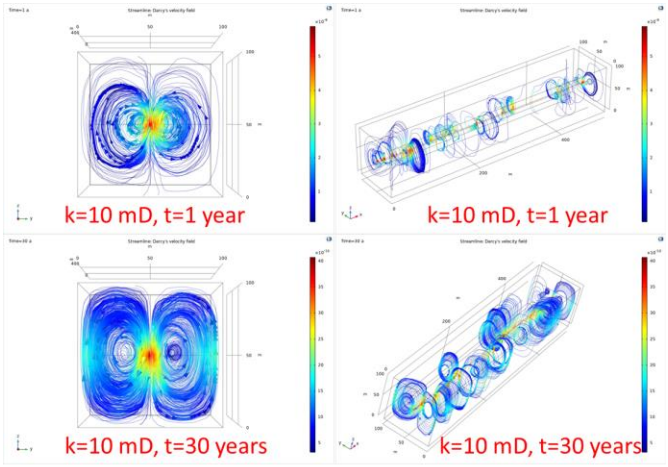

Figure 22: Velocity distribution and streamline at 1 year and 30 years of the case with 10 mD permeability.

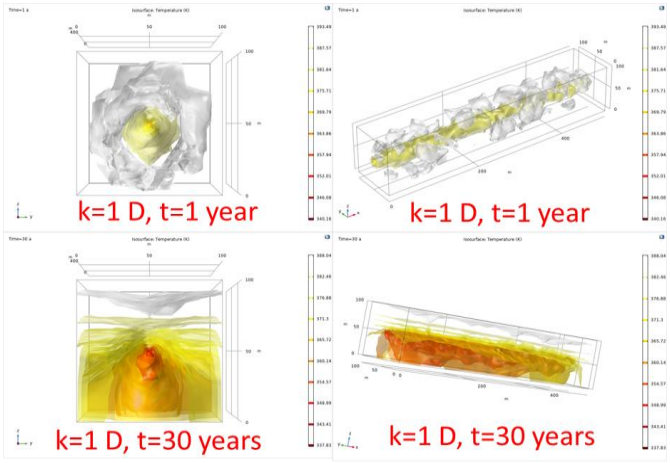

Figure 23: Temperature distribution at 1 year and 30 years of the case with 1 D permeability.

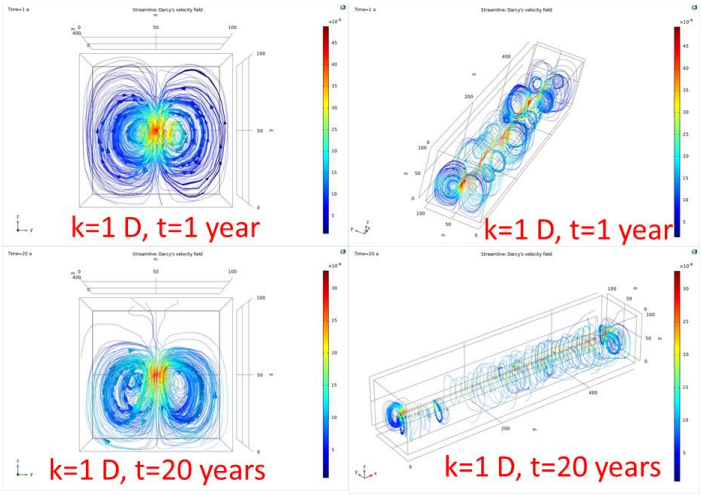

Figure 24: Velocity distribution and streamline at 1 year and 20 years of the case with 1 D permeability.

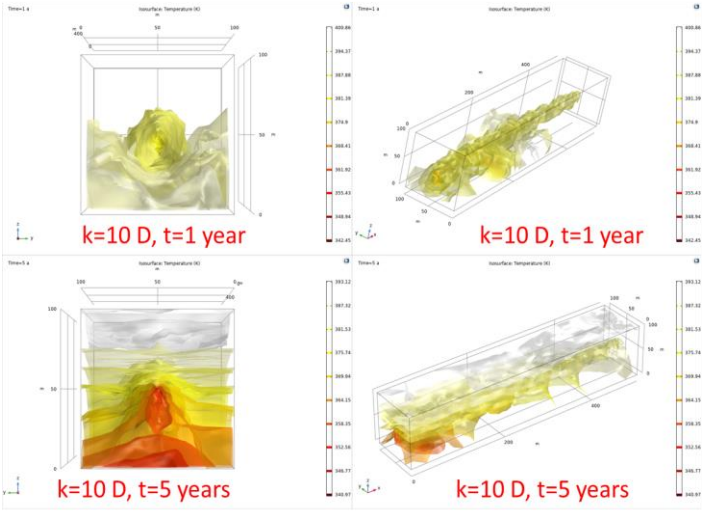

Figure 25: Temperature distribution at 1 year and 5 years of the case with 10 D permeability.

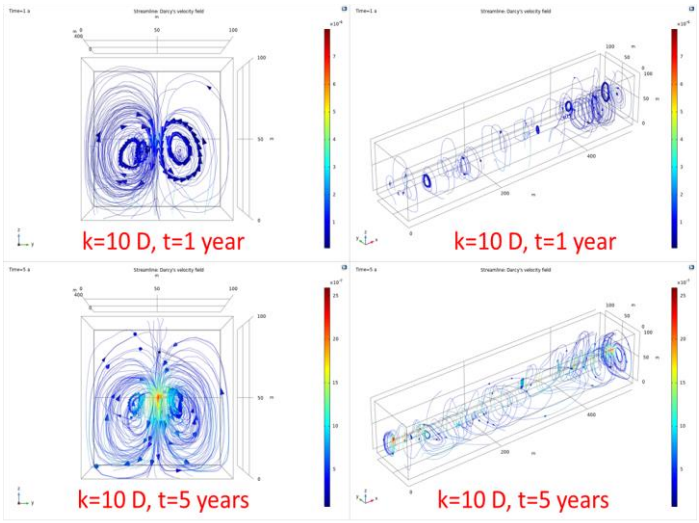

Figure 26: Velocity distribution and streamline at 1 year and 5 years of the case with 10 D permeability.

6. CONCLUSIONS

This study aims at investigating the effect of temperature decrease caused by the naturally induced density-driven convective flow in a closed-loop geothermal energy production system. Three analysis strategies have been applied to this problem. A patent-pending analytical method has been used to study the effect of the naturally induced convective flow velocity on overall heat transfer performance. By comparing and matching with pure heat conduction cases, pseudo-thermal conductivity could be evaluated to represent the heat transfer enhancement contributed by the naturally induced heat convection. A term defined as the degree of apparent conductivity enhancement, λ_E, is introduced in this work, with the empirical functions summarized under different induced convective flow velocity to showcase the appatent conductivity enhancement. The heat extraction performance from the closed-loop system is simulated by a local-grid-refined model using Flexwell setup in the CMG STARS module. Heat extraction performance can be largely enhanced by higher permeability starting from the range of 10 D ~ 100 D. The higher the effective permeability, the better the contribution from convective flow will be. But the enhancement is not obvious from the case with 0.001 mD permeability to the one with 1 D permeability. That could be because of the induced convective flow velocity increment is very limited in those cases. Another numerical model using finite element method by COMSOL was generated and analyzed for the naturally induced convective flow as well. A significant velocity improvement can be observed in the region near the horizontal wellbore, with the circle-loop convective flow pathways likely spreading outskirts in the lower region for the cases with higher permeability. The naturally induced convective flow velocity starts a significant increase in the permeability range of 1 D ~ 10 D, suggesting that only heavily fractured thermal reservoir does become sufficiently supportive to take the advantage of density-driven convective flow. Further evaluation for field cases is needed.

Based on the studies from these three methodologies, the effective thermal conductivity enhancement by naturally induced density-driven convective flow could be potentially significant for an operation over 30 years, affecting the long term fate of any geothermal project. This will be especially true for any geothermal project with highly permeable formations, naturally fractured reservoirs, and induced fractured region near horizontal wellbores. This kind of naturally induced convective flow will enhance the overall heat transfer performance of closed-loop geothermal energy production system. The pseudo-thermal conductivity term defined in this work could help generate an effective method to evaluate the local thermal properties for closed-loop system design.

Our future work will be extended to analytical modeling for 2D/3D geothermal reservoir, and integrating the fluid volume shrink, density-driven flow with dynamic viscosity change into the coupling process. The details of natural fractures or fracture network will be integrated into numerical model to study the fracture system features and their influence on induced convection flow. Empirical functions could be built to generate the relationship between the newly proposed apparent conductivity enhancement and overall reservoir permeability, which can be better applied in geothermal energy production practice.

REFERENCES

Amaya, A., Scherer, J., Muir, J., Patel, M., and Higgins, B.: GreenFire energy closed-loop geothermal demonstration using supercritical carbon dioxide as working fluid. 45th Workshop on Geothermal Reservoir Engineering, Stanford, CA, (2020), SGP-TR-216.

Beckers, K. F., Rangel-Jurado, N., Chandrasekar, H., Hawkins, A. J., Fulton, P. M., & Tester, J. W. (2022). Techno-Economic Performance of Closed-Loop Geothermal Systems for Heat Production and Electricity Generation. Geothermics, 100 (December 2021).

Blackwell, D.D., Steele J.L.: Thermal Conductivity of Sedimentary Rocks: Measurement and Significance. In: Naeser N.D., McCulloh T.H. (eds) Thermal History of Sedimentary Basins. Springer, New York, NY (1989). https://doi.org/10.1007/978-1-4612-3492-0_2.

Carslaw, H. S. and Jaeger, J. C.: Conduction of Heat in Solids, Oxford at the Clarendon Press (1959).

Dalla Santa, G., Galgaro, A., Sassi, R., Cultrera, M., Scotton, P., Mueller, J., Bertermann, D., Mendrinos, D., Pasquali, R., Perego, R., Pera, S., Di Sipio, E., Cassiani, G., De Carli, M., & Bernardi, A.: An updated ground thermal properties database for GSHP applications. Geothermics, 85 (2020), 101758. https://doi.org/10.1016/j.geothermics.

Eavor.: Eavor-Lite™ Demonstration Project. https://eavor.com/about/eavor-lite (2022).

Frind, E.O.: Simulation of long-term transient density dependent transport in groundwater. Advances in Water Resources, vol. 5, no. 2, (1982), 73–88.

Grasby, S.E., Allen, D.M., Bell, S., Chen, Z., Ferguson, G., Jessop, A., Kelman, M., Ko, M., Majorowicz, J., Moore, M., Raymond, J., and Therrien, R.: Geothermal Energy Resource Potential of Canada, Geological Survey of Canada, Open File 6914, (2011), 322 p. doi:10.495/288745.

GreenFire, https://www.greenfireenergy.com (2022).

Huyakorn, P.S., Andersen, P.F., Mercer, J.W., and White Jr., H.O.: Saltwater intrusion in aquifers: development and testing of a three-dimensional finite element model. Water Resources Research, vol. 23, no. 2, (1987), 293–312.

International Geothermal Association: What is geothermal? https://www.geothermal-energy.org/explore/what-is-geothermal/ (2021).

Kooi, H., Groen, J., and Leijnse, A.: Modes of seawater intrusion during transgressions. Water Resources Research, vol. 36, no. 12, (2000), 3581–3589.

Michael, H. A., Scott, K. C., Koneshloo, M., Yu, X., Khan, M. R., and Li, K.: Geologic influence on groundwater salinity drives large seawater circulation through the continental shelf. Geophysical Research Letters, vol. 43, no. 20, (2016), 10,782–10,791.

Newman, A. B.: Heating and cooling rectangular and cylindrical solids. Ind. and Eng. Chem. (28), (1936), 545.

Oldenburg, C.M., Pan, L., Muir, M.P., Eastman, A.D., Huggins, B.S.: Numerical Simulation of Critical Factors Controlling Heat Extraction from Geothermal Systems Using a Closed-Loop Heat Exchange Method. Lawrence Berkeley National Laboratory Recent Work. (2016). Permalink: https://escholarship.org/uc/item/4nj3s9ws.

Perm Inc.: Thermal Conductivity (Rock Core & Fluids). https://perminc.com/services/special-core-analysis-scal-lab-services/thermal-conductivity-rock-core-fluids/ (2021).

Rees, S.J., Spitler, J.D., Deng, Z., Orlo, C.D., & Johnson, C.N.: A study of geothermal heat pump and standing column well performance. Winter Meeting - Technical and Symposium Papers, American Society of Heating, Refrigerating and Air-Conditioning Engineers, 109, (2004), 1–10.

Schincariol, R.A. and Schwartz, F.W.: An experimental investigation of variable density flow and mixing in homogeneous and heterogeneous media. Water Resources Research, vol. 26, no. 10, (1990), 2317–2329.

Schincariol, R.A., Schwartz, F.W., and Mendoza, C.A.: On the generation of instabilities in variable density flow. Water Resources Research, vol. 30, no. 4, (1994), 913–927.

Simmons, C.T. and Narayan, K.A.: Mixed convection processes below a saline disposal basin. Journal of Hydrology, vol. 194, no. 1–4, (1997), 263–285.

Somerton, W.H.: Thermal properties of partially liquid saturated rocks at elevated temperatures and pressures. American Petroleum Institute Research Project Report 155, (1975). 35.

Stehfest, H.: Numerical Inversion of Laplace Transforms. Communications of ACM (1970) 13, No. 1, 47.

Stevens, J.D., Sharp Jr., J.M., Simmons, C.T., and Fenstemaker, T.R.: Evidence of free convection in groundwater: field-based measurements beneath wind-tidal flats. Journal of Hydrology, vol. 375, no. 3-4, (2009), 394–409.

Van Dam, R.L., Simmons, C.T., Hyndman, D.W., and Wood, W.W.: Natural free convection in porous media: first field documentation in groundwater. Geophysical Research Letters, vol. 36, no. 11, (2009).

Van Lopik, J.H., Hartog, N., Zaadnoordijk, W.J., Cirkel, D.G., & Raoof, A.: Salinization in a stratified aquifer induced by heat transfer from well casings. Advances in Water Resources, 86, (2015), 32–45. https://doi.org/10.1016/j.advwatres.2015.09.025

World Energy Council. World Energy Resources: Geothermal. (2013). https://www.worldenergy.org/assets/images/imported/2013/10/WER_2013_9_Geothermal.pdf.

Yan, M., Lu, C., Yang, J., Xie, Y., Luo, J., and Yu, X.: Impact of Low- or High-Permeability Inclusion on Free Convection in a Porous Medium. Geofluids, (2019). https://doi.org/10.1155/2019/8609682

Yuan, W.: Analytical Coupling Methodology of Fluid Flow in in Porous Media within Multiphysics Domain in Reservoir Engineering Analysis. Ph.D. dissertation, University of Regina. (2020).

Zhao, G., Yuan, W., Su, C., Jin, Y.: Analytical Simulation for Multiphysics and Multidomain Using Analytical Modeling Methodology. Canada Patent file reference number: 1672-002, (2021).